2021-01-0350

Evaluate the Effect of Seat Back Restriction on Head, Neck and Torso Responses of Front Seat Occupants when Subjected to a Moderate Speed Rear-Impact

Author, co-author (Do NOT enter this information. It will be pulled from participant tab in MyTechZone)

Affiliation (Do NOT enter this information. It will be pulled from participant tab in MyTechZone)

Abstract

During rear impacts, the front seats may rotate rearward due to occupant and seat momentum change leading to possibly large deformation of the seatback or even loss of occupant retention relative to the seat. One possible way of limiting this may be by introducing a structure that would restrict large rotations or deformations, however, such a structure would change the front seat occupant kinematics and kinetics. The goal of this study was to understand the influence of seat back restriction on head, neck and torso responses of front seat occupants when subjected to a moderate speed rear-impact. This was done by simulating a rear impact scenario with a delta-V of 37 km/h using LS-Dyna, with the GHBMC M50 occupant model and a manufacturer provided seat model. The study included two parts, the first part was to identify worst case scenarios using the simplified GHBMC M50-OS, and the second part was to further investigate the identified scenarios using the detailed GHBMC M50-O. The baseline condition included running the belted GHBMC on the seat at the specified pulse. This was followed by including a seatback constraint, a restriction bar, at 65 mm from the seat back to restrict rearward movement. Four different scenarios were investigated using the GHBMC M50-OS for the first part of the study both in the baseline and inclusion of a restriction bar behind the seatback: occupant seated normally; occupant offset on the seat; occupant rotated on the seat; and occupant seated normally but at a slightly oblique rear impact direction. The oblique condition was identified as the worst-case scenario based on the inter-vertebral kinematics; therefore, this condition was further investigated in the simulations with GHBMC M50-O. In the oblique rear impact scenario, the head missed the head restraint leading to inter-vertebral rotations exceeding the physiological range of motions regardless of the restriction bar use. However, adding a restriction bar behind the seat back showed a higher HIC and BrIC in both normal and oblique pulses due to the sudden stop, although the magnitudes were below the threshold.

Introduction

Rear impacts are less common and deadly for children than other crash modes [Viano and Parenteau 2008; Arbogast and Durbin 2013]. During vehicle rear impacts the front seat will deform rearward due to occupant and seat momentum change. It has been reported that the large deformation of the seatback of the front seat can occur and even possibly be collapsed during severe rear impact conditions [Sauders, 2003; Viano and Parenteau, 2008; Viano, 2009]. In impacts of sufficient change in velocity the seat back can intrude into the rear passenger zone. This could be prevented by restricting seat back rearward movement by increasing seat back stiffness or other secondary means which may cause issues to the front occupant. Restricting seat back movement can protect rear seat occupants by reducing a high magnitude impulse energy produced from the front seat and occupants, which can be transmitted to the rear passenger zone. However, it is unclear whether this seat back restriction will affect kinematics and kinetics of the front seat occupant negatively.

Since the whiplash injuries of front occupants in rear impact crashes are a serious problem, which cause enormous societal cost, investigation needs to be performed about influence of seat back restriction on cervical spine injury risk (e.g. whiplash) to front seat occupants. Claims of whiplash injuries in rear impact collisions are very common and costly, with estimates on the order of $2.7 billion annually in the United States [NHTSA, 2004]. The Insurance Institute for Highway Safety claims in 2007 that whiplash claims were 25 % of total payout for crash injuries. Whiplash injuries have also been identified as a serious problem in Europe and Asia. The United Kingdom estimates that there are 1500 whiplash claims file each day. 50% of vehicle collisions resulted in cervical spine injuries (e.g. whiplash) in Japan [Ono, 1996].

Biomechanical responses and possible whiplash injury risk of human subjects in rear impacts have been studied extensively using human volunteers [Ono, 1997; Croft and Philippens, 2007] and post-mortem human subjects [Mertz and Patrick, 1967; Yoganandan, 2000; Kang, 2015]. Most of the previous research have focused on low-to-moderate speed rear impacts (delta-V $\leq$ 25 km/h) and limited boundary conditions in their experiments.

Finite element (FE) human body models (HBM) are becoming more frequently utilized as a part of virtual testing to evaluate vehicle crashworthiness and to assess biomechanical responses and potentially injury risk to occupants [Jorlöv, 2017, Pipkorn, 2018, Ramachandra, 2019]. Anatomically representative FE models of the human body have been developed with great detail, such as the Global Human Body Model Consortium (GHBMC) models representing a 50th percentile male in a standard vehicle occupant seated posture [Gayzik, 2011]. The GHBMC models have been validated in several different scenarios at both body region and full-body levels, albeit mostly in frontal and side impact modes. At the body region level, the head-neck of this model has been validated in a rear impact scenario by comparing against volunteer data (peak acceleration 4g) and cadaver data (peak acceleration 7g) with rigid seatback [Fice, 2011]. More recently, the full body model has been evaluated in two moderate-speed rear impact scenarios (delta-V = 17

kph and 24 kph) by comparing against post mortem human subject (PMHS) data at the same impact severities. The model exhibited good biofidelity in the head to T1 region, which is of prime importance as far as rear-impact related injuries are concerned [Katagiri, 2019].

In rear impacts at low to moderate speed delta-V (~11 to 27kph), yielding seatbacks aid in reducing head accelerations and neck forces compared to non-rotating seatbacks [Viano, 2007]. Warner at al suggested that rigid seatbacks have the potential to increase exposure to injury in real world crashes. There are not sufficient data on kinematics and kinetics of the front occupant in the presence of a restriction device that would limit the seatback rotation and intrusion to the rear compartment when subjected to rear impact. In addition, such data would throw some light on the dynamic loads required to resist dynamic movement of the seat back in a moderate to high speed rear impact scenario. Therefore, the overarching objective of this study was to understand front seat occupant kinematics and biomechanical responses in rear impacts with and without the presence of such a restriction device using finite element (FE) simulations. The sub objectives included identifying occupant seating or loading scenarios that were potentially harmful to the head, neck and torso and quantifying front occupant response changes as a result of the restriction device compared to the seat without a restriction device.

Methods

The FE method approach included using the 50th percentile male GHBMC model to achieve the goals of this study. Figure 1 presents the technical approach used to conduct these investigations. The simulations were run using LS-Dyna v 971 MPP 9.01 (Livermore Software Technology Corporation, Livermore, CA) using 28 processors on the Owens cluster at the Ohio Supercomputer Center. Outputs from the simulations were analyzed using LS-prepost 4.5.17 (Livermore Software Technology Corporation, Livermore, CA). Data were acquired per standard SAE-J211, with the positive X directed from posterior to anterior, positive Y directed from left to right, and positive Z directed from superior to inferior.

The front seat model used in this study was identified and confirmed by running simulation using FE BioRID II ATD using IIHS protocol (IIWPG medium severity pulse) to ensure the neck loads were low (Figure 2). This effort was separate and outside the focus of this study.

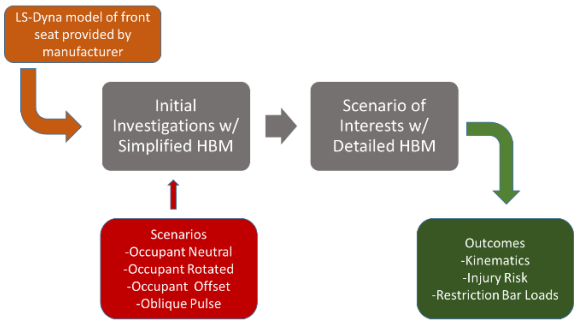

Figure 1. Methods flow-chart and technical approach

Figure 2. Selected FE front seat model

The first set of simulations for a given case were run with the occupant model seated on the selected seat and subjected to a generic rear impact pulse of approximately 19g (37kph/23.3mph) shown in Figure 3. The next set of simulations involved including a seatback constraint to restrict intrusion into the rear seat, called out as a restriction bar through the rest this document. This restriction bar was positioned at 65 mm from the seat back, which corresponds to an approximate b-pillar location with the seat-track all the way back

The GHBMC 50th percentile male simplified, and detailed models were used in this study. The height and the weight of the models are 1.75m and 78.5kg respectively.

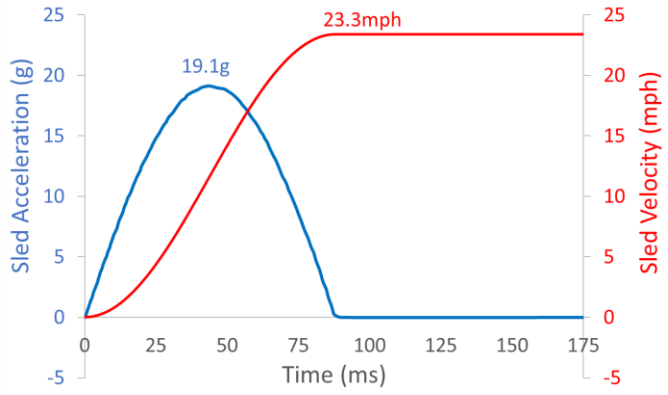

Figure 3. Rear impact pulse used in the study

Simulations with GHBMC 50th Simplified Male

A preliminary parametric study was performed to identify high injury severity cases using the GHBMC 50th male simplified occupant model (GHBMC M50-OS v2.0). This model is considerably less

computationally expensive compared to its detailed counterpart, while producing equivalent gross kinematics. The GHBMC M50-OS has approximately 150,000 deformable elements and its modularity is similar to ATDs, making it easy to position.

Positioning of the GHBMC M50-OS limbs was achieved using the limb positioning function in LS-Prepost, and head was rotated around the occipital condyle joint in the sagittal plane until the Frankfort plane was horizontal, by performing positioning simulation applying a prescribed motion. The backset (distance between the head and the head restraint and the topset (distance between the head center of gravity and the top of the head restraint), were set to 5 mm and 62 mm respectively, as shown in Figure 4.

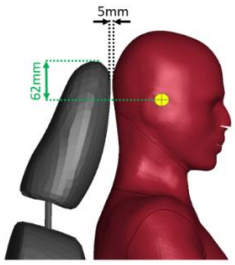

Figure 4. Backset and topset measurements

Seatbelt fitting tool was used to route the shoulder and lap belts, which were modeled as a combination of 2D triangular shell elements and 1D beam elements. A retractor was defined at the D-ring to pretension the belt segments and maintain the same tension by spooling out zero length beam elements at the D-ring or spooling in 1D beam elements just outside the retractor. A slip ring was defined at the point of contact between the 1D beam elements of the shoulder and lap belts to allow for smooth transitioning to either side during maintenance of the belt tension. Contact definitions were added to the model setup using the CONTACT_AUTOMATIC_SURFACE_TO _SURFACE command between the exterior skin of the GHBMC and the environment, as well as between the skin and belt segments. A frictional coefficient of 0.3 was selected for the contact definitions. The pre-impact position of the GHBMC M50-OS without and with restriction bar are shown in Figures 5a and 5b respectively.

Figure 5a. Pre-impact position of the GHBMC M50-OS without restriction bar

Figure 5b. Pre-impact position of the GHBMC M50-OS with restriction bar

Four different scenarios were investigated using the GHBMC M50-OS for this part of the study both in the presence and absence of a restriction bar behind the seatback: baseline, right offset, right rotated and oblique (Figure 6). Each scenario is described below.

Baseline: The sled was constrained in all degrees-of-freedom (DOF) except translation in the global X direction. A sled pulse was prescribed to the floor using the BOUNDARY_PRESCRIBED_ MOTION_RIGID command.

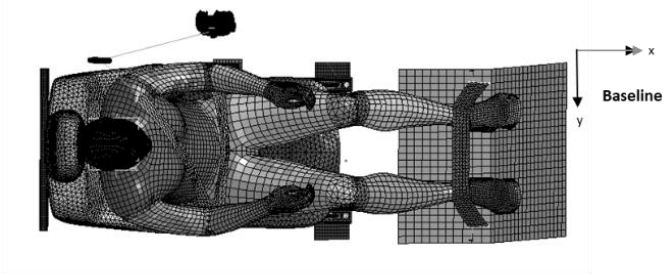

Figure 6a. GHBMC M50-OS in baseline scenario, sled pulse X-direction

Right Offset: The GHBMC was translated and positioned 30 mm to the right along the global y-axis. The same sled condition as the baseline case was used.

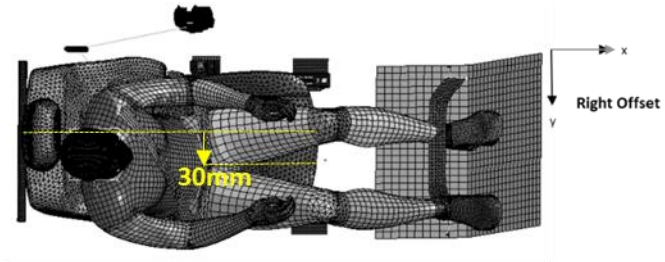

Figure 6b. GHBMC M50-OS in right offset scenario, sled pulse X-direction

Right Rotated: The GHBMC was rotated to the right by 30 degrees about the global z-axis. The same sled condition as the baseline case was used.

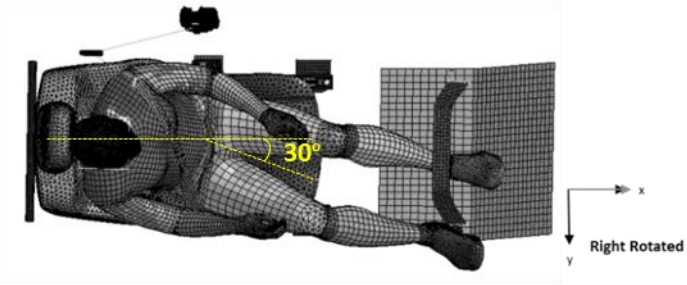

Figure 6c. GHBMC M50-OS in right rotated scenario, sled pulse X-direction

Oblique: The GHBMC was seated in the same position as the baseline case, but the sled pulse was applied along a vector 30 degrees clockwise from the global x-axis, defined using the DEFINE_VECTOR command. The sled translational constraint along global y-axis was removed to allow the sled to move in the x-y plane, as compared to the previous three cases.

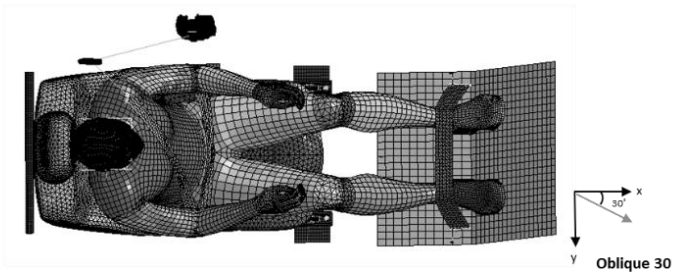

Figure 6d. GHBMC M50-OS in oblique scenario (seating same as baseline), sled pulse 30deg to X-direction in XY plane

Gross kinematics were measured in the body fixed coordinate systems (SAE-J211). The detailed kinematics such as head to T1 rotations (difference between head rotation in a given axis and corresponding T1 rotation) and intervertebral rotations (difference of rotation between the upper adjacent vertebra and lower adjacent vertebra in a given axis) were measured in local coordinate systems created on the anterior superior aspect of each vertebrae as shown in Figure 7.

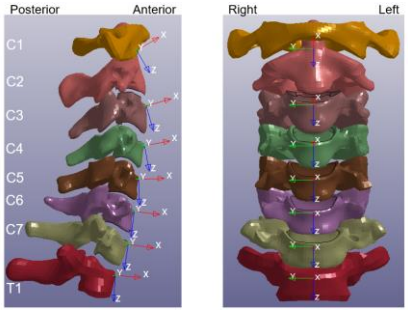

Figure 7. Local coordinate systems created for intervertebral kinematics

Simulations with GHBMC 50th Detailed Male

The next part of the study involved in investigating further the scenarios of interest, partially based on outcomes from simplified simulations using the GHBMC 50th male detailed occupant (GHBMC M50-O v5.0). The detailed GHBMC was developed to simulate tissue-level injury response in addition to gross kinematics. This model has a finer mesh with approximately two million deformable elements and has shown to have better biofidelity than its simplified counterpart in all body regions. The GHBMC M50-O has deformable cervical vertebrae, deformable discs, and 1D elements representing muscles and ligaments. It also includes anatomically accurate muscle groups and subcutaneous tissue represented by 3D elements.

Positioning the detailed model is more complicated than the simplified model due to absence of dummy-like modularity. Positioning the limbs was performed using multiple steps of positioning simulations. The head and the limbs were rotated around their corresponding joints by applying a prescribed motion while constraining any deformation of the other body regions. The GHBMC was placed on the seat cushion foam using a seating simulation, where a gravity load was applied until the model settled on the seat.

The two scenarios investigated in this part of the study included baseline and oblique with and without restriction bars (Figure 8). The positioning of the GHBMC was the same across all four cases.

Figure 8. Pre-impact position of the GHBMC M50-O with Restriction Bar

Results

A total of 12 simulations were run, eight with the simplified GHBMC and four with the detailed GHBMC. Generally, as the sled moved forward, the thorax of the occupant moved backward pushing onto the seatback followed by the head and neck contacting the head restraint. In the cases without the restriction bar, the occupant ramped up along the seatback with the head-neck wrapping around the head restraint. This was generally true unless the head contact was only partial, such as in oblique pulse or right offset scenarios, in which case there was a twisting motion of neck and torso introduced. In cases where the seatback intrusion into the rear compartment was restricted, the occupant experienced rebound with less ramp-up compared to no restriction bar scenarios.

Simulations with GHBMC 50th Simplified Male

The peak translations and rotations of the head relative to first thoracic vertebrae (T1) along with the time of occurrence are tabulated in Table 1. The bold and italicized values show the maximum value in a given column for both with and without bar conditions. For example, the right offset without bar and oblique with bar conditions experienced the highest head displacement w.r.t T1 in X-direction. The greater X and Z rotations in both the right offset and oblique conditions suggest head-neck twist after contacting head-restraint. The intervertebral kinematics as magnitude comparisons of displacements and rotations are provided in Appendix A.

Table 1. Peak translations and rotations of head relative to T1

Scenario		Displacement - *mm (ms)*			Rotation - *deg (ms)*		
		X	Y	Z	X	Y	Z
Baseline	w/ bar	-39.4 (120.9)	20.4 (134.7)	16.9 (67.3)	5.7 (137.9)	-21.3 (72.2)	-2.9 (102.9)
	w/o bar	-63.5 (158.5)	-7.7 (174.2)	11.0 (162.8)	-7.5 (174.9)	23.9 (138.7)	-6.9 (155.2)
Right Offset	w/ bar	-58.0 (130.2)	***40.2 (139.9)***	22.0 (131.6)	***33.5 (140.1)***	21.8 (129.7)	31.2 (129.7)
	w/o bar	***-124.3 (174.9)***	22.4 (123.3)	52.5 (174.9)	22.8 (174.9)	***52.5 (174.4)***	***26.7 (174.9)***
Right Rotated	w/ bar	-46.4 (131)	21.0 (79.6)	19.7 (72.9)	-7.4 (135)	-20.2 (76.6)	14.3 (85.8)
	w/o bar	-53.7 (145)	-12.9 (172)	10.8 (165)	-9.5 (175)	22.5 (145)	-7.8 (163)
Oblique	w/ bar	***-124.4 (144.1)***	-35.7 (139.4)	***63.1 (139.9)***	-16.2 (125.5)	***66.2 (146.1)***	***-34.3 (106.5)***
	w/o bar	-99.4 (142.5)	***-37.8 (136.2)***	***37.1 (142.5)***	***-25.6 (142.5)***	32.1 (142.5)	-12.2 (142.5)

The values of head injury criterion (HIC) and brain injury criterion (BrIC) are plotted in Figure 9. The HIC values were much lower than the threshold in all cases. However, the BrIC reached injury assessment reference value (IARV) for the right offset with bar scenario due to the head experiencing rotation at higher angular velocities upon contacting the edge of head restraint.

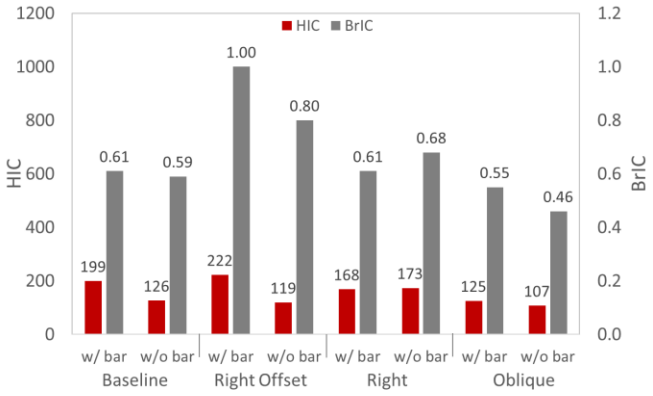

Figure 9. Restriction Bar Forces

Figure 10 shows the comparison of peak forces measured on the restriction bar. The forces were similar across all load cases, although the oblique case showed a lower magnitude. This is possibly due to the twisting of the seat as the head moved away from the head restraint and the weight of the GHBMC was more concentrated to the left side of the seat back.

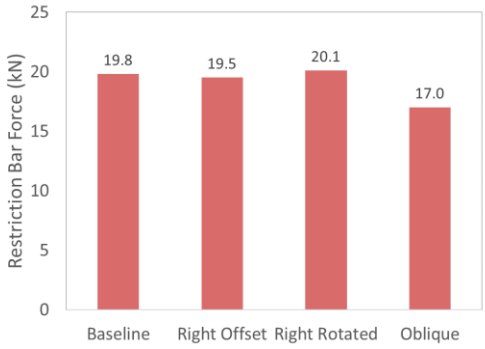

Figure 10. Restriction Bar Forces

Simulations with GHBMC 50th Detailed Male

Figure C1 shows the different phases of motion for the GHBMC M50-O in the four different cases. The initial position of the GHBMC was same in all four cases. The head contact with the head-restraint occurred at the same time in these cases. The baseline without restriction bar simulation shows a typical occupant kinematics in rear impact sled tests, while the baseline with restriction bar shows less movement of the occupant in both x-and z-directions, indicating that the GMBMC translated into the seatback and dissipate energy. For the oblique without restriction bar condition, the head restraint and seatback showed twist motions, which can increase risk of injuries on the neck and possibly thorax. The oblique with restriction bar shows similar whole body kinematics as the baseline with restriction bar condition until 67.5 ms and then indicates neck twist around 100 ms.

Figure 11 shows the head trajectories in the XZ plane for all four conditions simulated with the GHBMC M50-O. For the with bar cases, the head starts rebounding around -250 mm of X excursion after contact with head restraint. However, the head moves upward and forward in baseline compared to lower and forward in oblique.

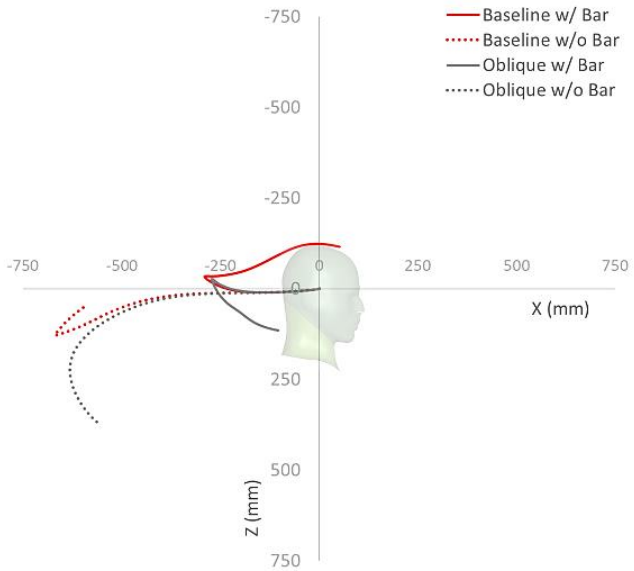

Figure 11. Restriction Bar Forces

The bar plot in Figure 12 shows comparisons of head relative to first thoracic vertebrae (T1) rotations. The head to T1 rotations about all three axes were higher in the oblique conditions than the baseline conditions, which indicates higher chance of the neck injury risk in the oblique conditions. Figures 13 shows intervertebral rotations about y-axis. The intervertebral rotations at the C2-C3 through C6-C7 exceeded physiological range of motions (ROM) in the oblique conditions, but only one level at C3-C4 exhibits higher intervertebral rotation in the baseline conditions. Figure 14 shows intervertebral axial forces. Although kinematic outcomes were smaller in the baseline conditions than the oblique conditions, the intervertebral forces were greater in the baseline conditions, especially with restriction bar, than the oblique conditions.

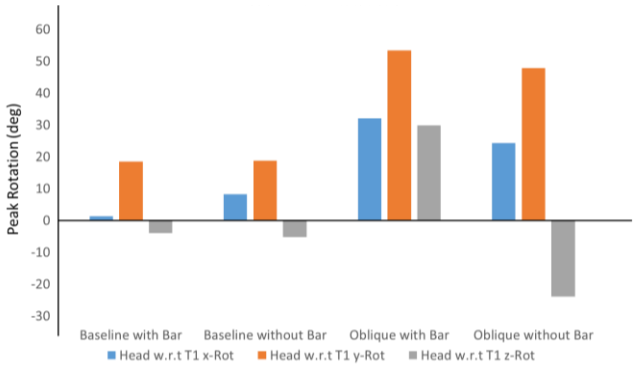

Figure 12. Magnitude comparisons: Head relative to T1 rotations

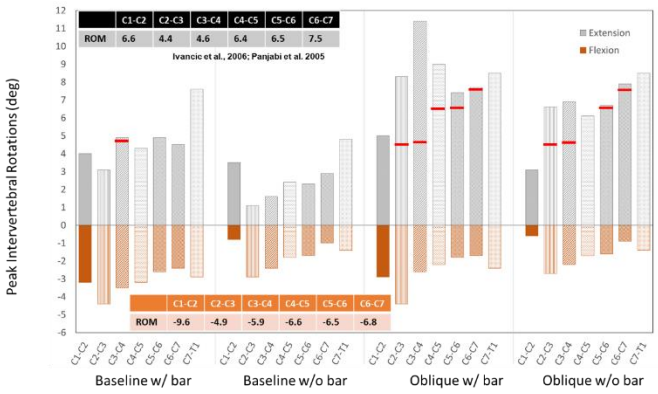

Figure 13. Magnitude comparisons: Intervertebral rotations about Y (Threshold values listed in boxes and marked with a red line)

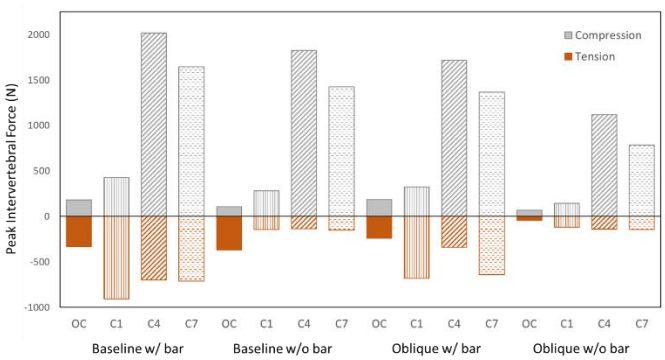

Figure 14. Magnitude comparisons: Intervertebral forces

The head, T1 and intervertebral kinematics as time-history plots are provided in Appendix B. Generally, the intervertebral motion was observed after head contact with head restraint.

Figure 15 shows the restriction bar forces measured as contact force between the seatback and the bar. The reaction force in the baseline condition was higher than that in the oblique condition since the GHBMC exhibited lateral motions in the oblique condition.

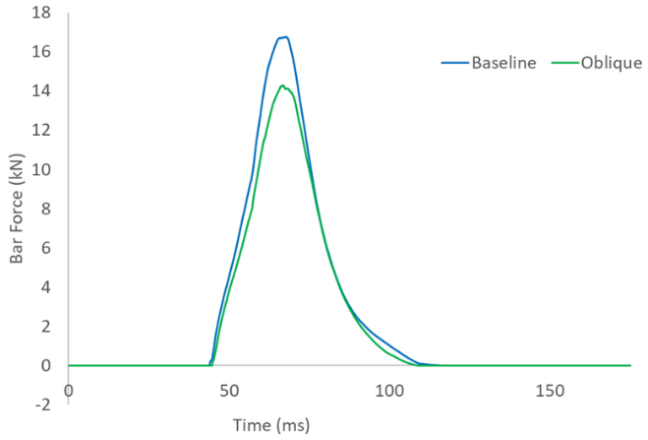

Figure 15. Restriction bar forces

The HIC and BrIC were calculated from the head accelerations and angular velocities and are presented in Figure 16. Even though both HIC and BrIC values were well below injury thresholds, the baseline with restriction bar condition had higher HIC and BrIC values than the other conditions.

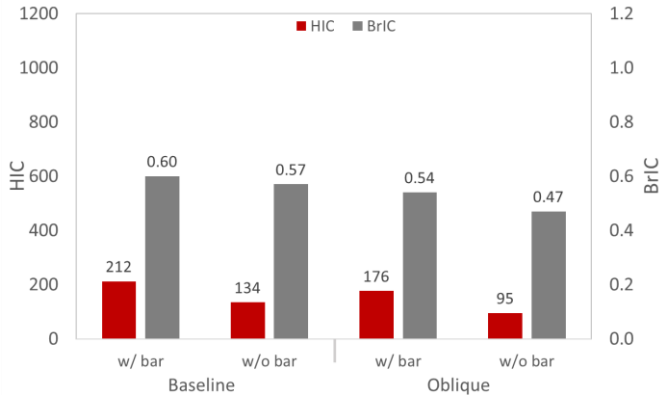

Figure 16. Magnitude comparisons: HIC and BrIC

In addition to the head and neck kinematics, rib fractures were evaluated based on cortical bone failure strain criteria (0.018/s) and are shown in Figure 17. For both baseline and oblique conditions without restriction bar, yielding and pocketing of the seat back absorbed energy well so that no rib fractures occurred. However, for the baseline condition with restriction bar, rib fractures occurred at 8th rib. Due to combination of stress concentration from restricting the seat back movement and thorax twist induced from the oblique sled input, rib fractures occurred more in the oblique condition with restriction bar than the other conditions.

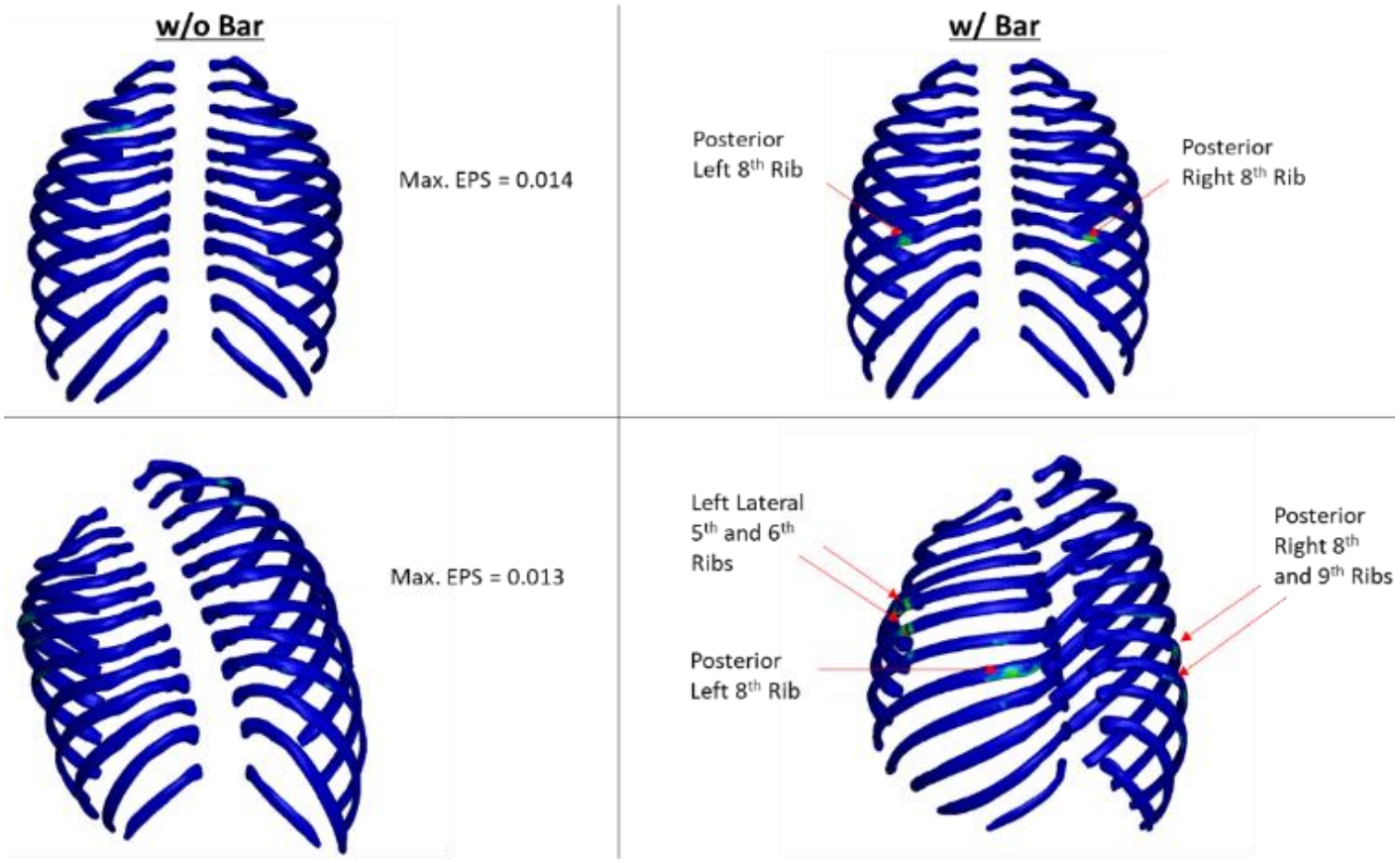

Figure 17. Rib-fractures observed in the GHBMC M50-O simulations [Top Row] Baseline; [Bottom Row] Oblique

Discussion

The objective of this study was to understand the driver seat occupant head, neck and torso responses in a moderate speed rear impact scenario in the presence of a seatback restriction device. This was done analytically by subjecting a belted GHBMC seated on a production seat to a 19g rear impact pulse with and without a seatback restriction bar. This effort was extended to also perform these simulations when the same 19g pulse was oriented obliquely at a 30degree vector. Injuries from rebound in rear impacts have been studies extensively in the past. Schimmer and Wolf (1961) found that non-rotating seats increased the risk for occupant rebound into front interior for unbelted occupants, suggesting greater rebound from seats that remain upright in rear impacts. Digges (1993) found that the most significant source of harm was neck injuries not related to direct loading, followed by contact to head restraint and forward components. In this current study, head rebound velocities were measured relative to the sled and these are plotted in Figure 18.

In the case of baseline with bar, the head velocity first increased in the opposite direction of the sled motion until after head contact that occurs at around 60ms, and quickly changes direction reaching a peak rebound velocity of 5.2 m/s after head release. A similar trend is observed in the case of oblique with bar, albeit reaching a velocity of only 1.2 m/s soon after head release but eventually reaching 3.3 m/s as the head rotates laterally and away from head-restraint.

In the without bar cases for both baseline and oblique, the head velocities first increased in the opposite direction of the sled due to ramping of the subject followed by the head extending over top of the head restraint and continued rearward rotation, consistent with Viano (2013) findings. The peak head rebound velocity for the unrestricted baseline case was 3.8 m/s at the time of simulation termination, which was lower than the values reported in the Viano (2013) study for the 20 mph tests with Hybrid III ATD. So it is possible that a longer simulation time could show a slightly higher peak rebound velocity, although the values need to be confirmed with studies using human subjects or ATDs specifically designed for rear-impact investigations.

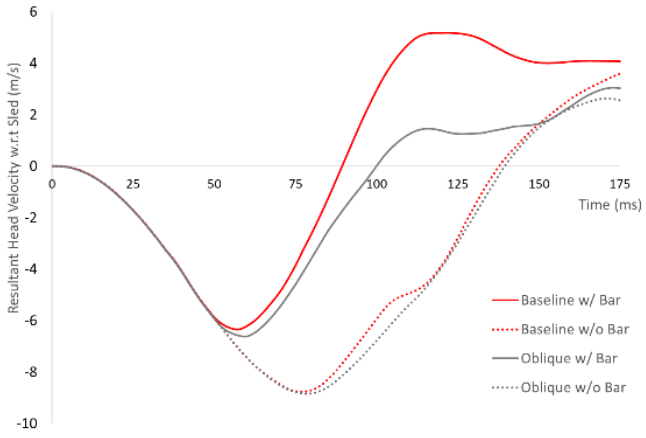

Figure 18. Head velocities relative to sled

Viano and Parenteau (2008) found from their investigations of FMVSS301 rigid barrier tests that the average biomechanical responses for head were below IARVs for front seat occupants. The HIC values are similar to those reported in the Viano and Parenteau (2008) and Viano (2013) studies. The Moorhouse (2012) studies have similar HIC values for the low/moderate speed impact, but it may be a metric that needs to be reevaluated for high speed scenarios.

The BrIC for the front seat occupant, when experiencing rear and oblique-rear impacts ranged from 47 to 60% of the threshold value. The BrIC takes into account the angular velocities of all three directions, and it is suggested in the Kitagawa (2017) study that higher degree of obliqueness gave higher BrIC values in rear impacts. The obliqueness between seating and impact directions increases the Z-component of angular velocity, which increases the BrIC value. In the current study, the oblique rear impact resulted in slightly lower values than the pure rear impact scenarios, however, a partial contact with the head restraint in pure rear impact that increased the head neck twist increasing the Z-component of the angular velocity. So it is possible that the obliqueness was insufficient to increase BrIC in the oblique rear scenario.

Rib fractures were found at the locations of the restriction bar due to high stress concentration, although seat foam and frame absorbed energy (Figure 19). In high speed rear impacts, rib fractures could be one of the major injuries if the seat back is too stiff. Although information on injury in high speed rear impacts is very limited in the literature, one previous study, in which they inspected German In-Depth Accident Study (GIDAS), found that rib fractures occurred in a high-speed rear impact condition [Zellmer, 2018]. Rib fractures were also found and documented in a recent PMHS study [Kang, 2020]. The interaction between the PMHS thorax and seat frame structure, such as shoulder belt retractor structure in an all belts to seat (ABTS), was the main source of the rib fractures in the 25 degree recline seat back condition using a rigidized production seat. It is important to find an optimal balance between seat frame stiffness and seat back properties to mitigate injury risk on thorax in high speed rear impacts. Adding the restriction bar or rigidizing seat frame increased likelihood of rib fractures. An interesting finding from this study is the increase of the likelihood of rib fractures in the oblique scenario. Higher compressive strain on the left posterior aspect of the ribs were found in this study. The twist motion of the thorax in the oblique scenario resulted in asymmetric compression force on the left side of the thorax, which was interacted with the left side of the seat back side bolstering (Figure 20). Further investigation should be made to ensure whether this asymmetric loads on the thorax due to the twist motion is the potential injury mechanism of the rib fractures in oblique rear impacts.

The fracture prediction capability of the GHBMC M50-O may be attributed to several factors such as material property, geometry, failure strain, cortical thickness distribution etc. The model uses variable thickness shell elements for cortical bone of ribs, with thicknesses ranging from 0.2 to 2.7 mm. The rib is defined by an elastic-plastic material property, with plastic failure defined at 1.8% and 13% plastic strain for the cortical and trabecular bones, respectively. These values are representative of a 50 year old occupant [Golman, 2014]. Although the model is validated for thoracic responses, the exact fracture locations and frequency observed in this study may be confirmed by conducting experiments with PMHS.

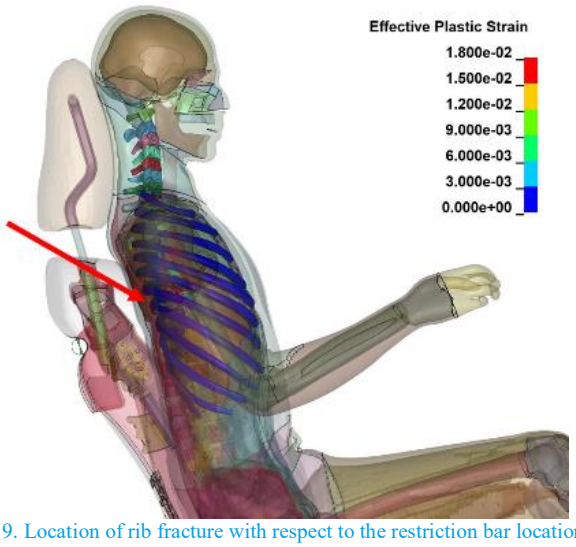

Figure 19. Location of rib fracture with respect to the restriction bar location in baseline condition [right side view]

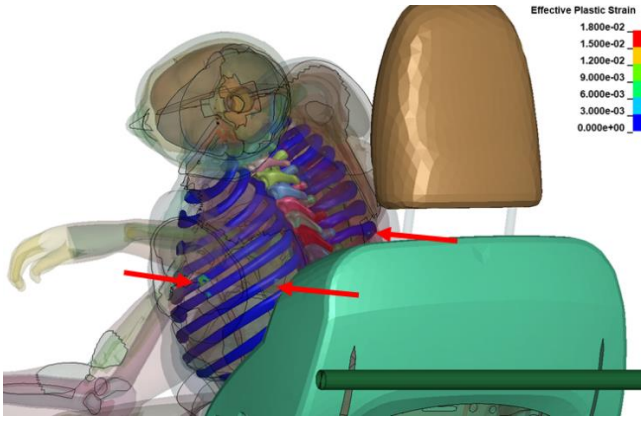

Figure 20. Location of some of the rib fractures in oblique w/ bar condition [left rear oblique view]

With the inclusion of a restriction device behind the seatback, the magnitude and rate of loading on the restriction bar for the baseline case was greater compared to the oblique case, since the principle direction of force was purely X and the seatback rotation occurred majorly about Y-axis. But in the Oblique case, the seatback starts to twist to the left and the occupant starts to rotate about the negative Z. Therefore, instead of the seatback contacting the restriction bar evenly, the left part of seatback contacts first followed by mass accumulation from inertial and occupant loading, leading to a slightly lower rate of loading and magnitude.

Limitations

The primary limitation of the study is the validity of the entire model including the GHBMC occupant and environment, due to the lack of similar PMHS studies for comparison. Although the GHBMC and the seat have been validated separately, the outcomes seen in the study may be sensitive to GHBMC positioning. However, this has been performed based on experience in both PMHS sled testing and other sled-based simulations with GHBMC.

Studies have suggested stiffening the front seatbacks to prevent rearward rotation into second row seat in rear impacts. Viano and

Parenteau (2008) found that stiffening seatback would increase the risk to second row child occupants in frontal crashes. While this current study investigated a restriction device installed behind the seatback instead, further evaluation is required to see if the risk suggested by Viano is mitigated or otherwise.

Finally, this study by no means intends to suggest the use of a restriction bar behind seat back or otherwise and is simply meant to provide information based on FE simulations as to what the occupant might experience under the constraints chosen in this study. The results presented are limited to the occupant and restraint parameters and warrants further evaluation by changing the impact direction, crash pulse, location of restriction device and seat models.

Summary/Conclusions

The objective of this study was to understand front seat occupant kinematics and biomechanical responses of the head, neck and torso with and without the presence of seatback restriction device when subjected to moderate to high speed rear impact,. This was done by simulating rear and oblique rear impact scenarios with a delta-V of 37 km/h using GHBMC models and an IIHS protocol satisfied seat model for low neck loads. The study included two parts, the first part was to identify worst case scenarios, including occupant seating and direction of pulse, for head-neck responses using the simplified GHBMC model. the second part was to further investigate the rear and oblique rear impact using the detailed GHBMC model.

A total of twelve simulations are presented in this study: eight using GHBMC M50-OS and four using GHBMC M50-O detailed model. Some of the key findings are listed below.

1. Adding a restriction bar behind the seat back resulted in higher HIC and BrIC values due to the sudden stop. The restriction bar also increased the risk of rib-fractures sustained by the occupant as the torso pressed against the constraint.
2. In the oblique rear and the right offset occupant seating scenarios, the head contacted the head restraint partially, resulting in intervertebral rotations exceeding physiological range of motions regardless the restriction bar use.
3. The maximum head rebound velocity occurred in the restricted condition, where the stored energy from seat deformation and chest restraint combined to give a head forward velocity relative to the sled.
4. The oblique rear impact with restriction bar had higher number of rib fractures likely due to the combination of inertial loads induced from the thorax mass and twisting phenomenon of the occupant applied to the seat back bolstering. Optimal yielding and pocketing properties of the seat back may be investigated further to prevent rib fractures in the moderate-to-high speed rear impacts.

References

1. Arbogast K.B., Durbin D.R. (2013) Epidemiology of Child Motor Vehicle Crash Injuries and Fatalities.
2. Croft A, Philippens M. The RID2 Biofidelic Rear Impact Dummy: A Pilot Study Using Human Subjects in Low-Speed Rear Impact Full Scale Crash Tests. J. Accident Analysis and Prevention, 2007, 39: pp. 340-346.
3. Digges, K., Morris, J., & Malliaris, A. (1993). Safety Performance of Motor Vehicle Seats.
4. Fice, J. B., Cronin, D. S., & Panzer, M. B. (2011). Cervical spine model to predict capsular ligament response in rear impact. Annals of biomedical engineering, 39(8), 2152-2162.
5. Gayzik FS, Moreno DP, Vavalle NA, Rhyne AC, Stitzel JD. (2011) Development of the Global Human Body Models Consortium mid-sized male full body model. Injury Biomechanics Research Workshop, 2011.
6. Golman AJ, Danelson KA, Miller LE, Stitzel JD. Injury prediction in a side impact crash using human body model simulation. Accid Anal Prev. 2014.
7. Kang et al**.,** Biomechanical Responses and Injuries of PMHS in Rear Facing Alternative Seating Configurations, SAE Government/Industry Meeting, 2020
8. Kang Y, Moorhouse K, Icke K, Stricklin J, Herriott R, Bolte JH. Rear impact head and cervical spine kinematics of BioRID II and PMHS in production seats. International Conference on the Biomechanics of Impact (IRCOBI), 2015, IRC-15-38.
9. Katagiri M, Zhao J, Lee S, Moorhouse K, Kang YS "Biofidelity Evaluation of GHBMC Male Occupant Models in Rear Impacts", IRCOBI 2019.
10. Kitagawa Y, Hayashi S, Yamada K, Gotoh M. Occupant Kinematics in Simulated Autonomous Driving Vehicle Collisions: Influence of Seating Position, Direction and Angle. Stapp Car Crash J. 2017
11. Koppel, Sjaan & Octavio, Jesús & Bohman, Katarina & Logan, David & Raphael, Wassim & Jimenez, Leonardo & Lopez-Valdes, Francisco. (2019). Seating configuration and position preferences in fully automated vehicles. Traffic Injury Prevention. 20. 1-7. Pipkorn 2018
12. Mertz HJ, Patrick LM. Investigation of the Kinematics and Kinetics of Cervical Spine. J. Stapp Car Crash. 1967, 11, SAE Paper No. 670919.
13. Moorhouse, K., Donnelly, B., Kang, Y. S., Bolte IV, J. H., & Herriott, R. (2012). Evaluation of the internal and external biofidelity of current rear impact ATDs to response targets developed from moderate-speed rear impacts of PMHS. SAE Technical Paper; 2012 Oct 29.
14. NHTSA, Federal Motor Vehicle Safety Standards; Head Restraints (FMVSS 202a), Federal Register 49 CFR Part 571, Docket no. NHTSA-2004-19807, December 14, 2004.
15. Ono K, Kaneoka K, Wittek A, Kajzer J. Cervical Injury Mechanism Based on the Analysis of Human Cervical Vertebral Motion and Head-Neck-Torso Kinematics During Low-Speed Rear Impacts. J. Stapp Car Crash. 1997, 41, SAE Paper No. 973340.
16. Ono K, Kanno M. Influence of the Physical Parameters on The Risk to Neck Injuries in Low Impact Speed Rear-End Collisions. Accid Anal Prev 1996, 28: pp. 493-499.
17. Ramachandra R, Kang YS, Bolte J, Murach M, Moorhouse K, Stammen J, Agnew A "Evaluation of Skeletal and Soft Tissue Contributions to Thoracic Response of GHBMC M50-O Model in Dynamic Frontal Loading Scenarios", IRCOBI 2019.
18. Viano DC, Parenteau CS, Burnett R. Rebound after rear impacts. Traffic Inj Prev. 2013
19. Viano DC, Parenteau CS, Burnett RA, James MB. Influence of Seating Position on Dummy Responses with ABTS Seats in Severe Rear Impacts. SAE Technical Paper; 2009
20. Viano DC, Parenteau CS, Prasad P, Burnett R. Stiff versus Yielding Seats: Analysis of Matched Rear Impact Tests. SAE 2007-01-0708, Society of Automotive Engineers, Warrendale PA, 2007.Schimmer and Wolf (1961)
21. Viano DC, Parenteau CS. Serious injury in very-low and very-high speed rear impacts. SAE Technical Paper; 2008 Apr 14.
22. Yoganandan N, Pintar F, Stemper B, Schlick M, Philippens M, Wismans J. Biomechanics of Human Occupants in Simulated

Rear Crashes: Documentation of Neck Injuries and Comparison of Injury Criteria. J. Stapp Car Crash. 2000, 44, SAE Paper No. 2000-01-SC14.
23. Zellmer, H., Lubbe, N., & Sander, U. (2018). Assessing the Injury Risk of Car Occupants on Rearward Facing Seats–An Analysis of GIDAS Cases. In 8th ESAR Conf. Hannover, Germany.

Definitions/Abbreviations

ATD	Anthropomorphic test device
BrIC	Brain Injury Criteria
C#	Cervical vertebrae number
DV	Delta-V, change in velocity
EPS	Effective plastic strain
FE	Finite element.
GHBMC	Global Human Body Models Consortium
HBM	Human body models
HIC	Head Injury Criteria
HIII	Hybrid-III ATD
NHTSA	National Highway Traffic Safety Administration
PMHS	Post mortem human subjects
SAE	Society of Automotive Engineers
T#	Thoracic vertebrae number

Appendix A - GHBMC M50-OS (Simplified) Model Responses

Figure A1. Magnitude comparisons: Anterior intervertebral x-direction displacements in mm

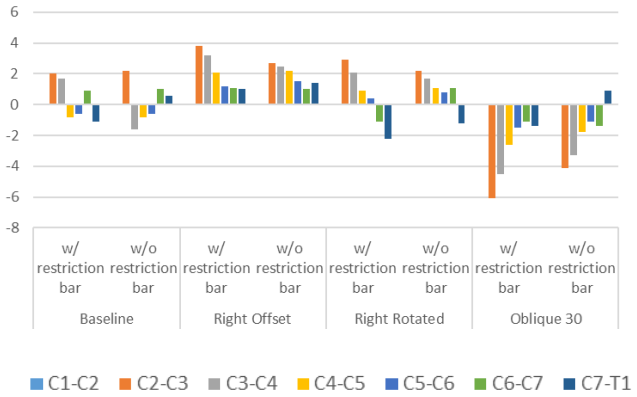

Figure A2. Magnitude comparisons: Anterior intervertebral y-direction displacements in mm

Figure A3. Magnitude comparisons: Anterior intervertebral z-direction displacements in mm

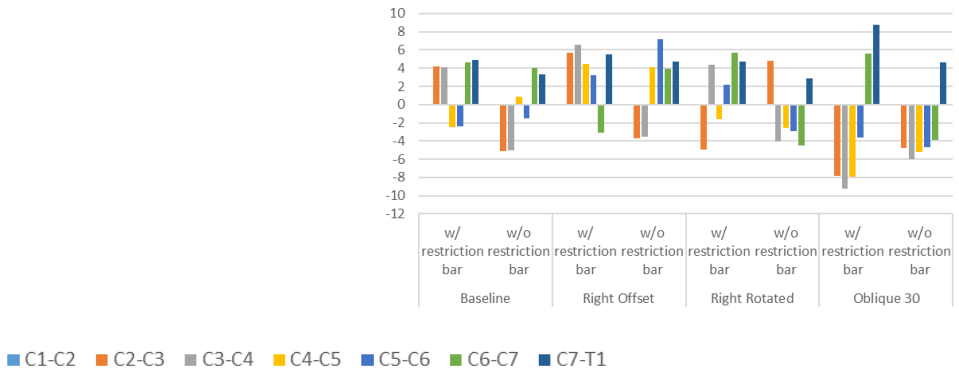

Figure A4. Magnitude comparisons: Anterior intervertebral x-direction rotations in deg

Figure A5. Magnitude comparisons: Anterior intervertebral y-direction rotations in deg

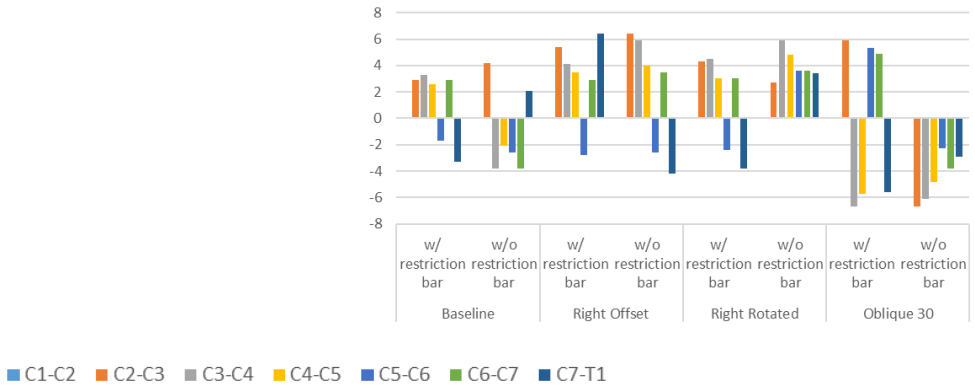

Figure A6. Magnitude comparisons: Anterior intervertebral z-direction rotations in deg

Appendix B – GHBMC M50-O (Detailed) Model Responses

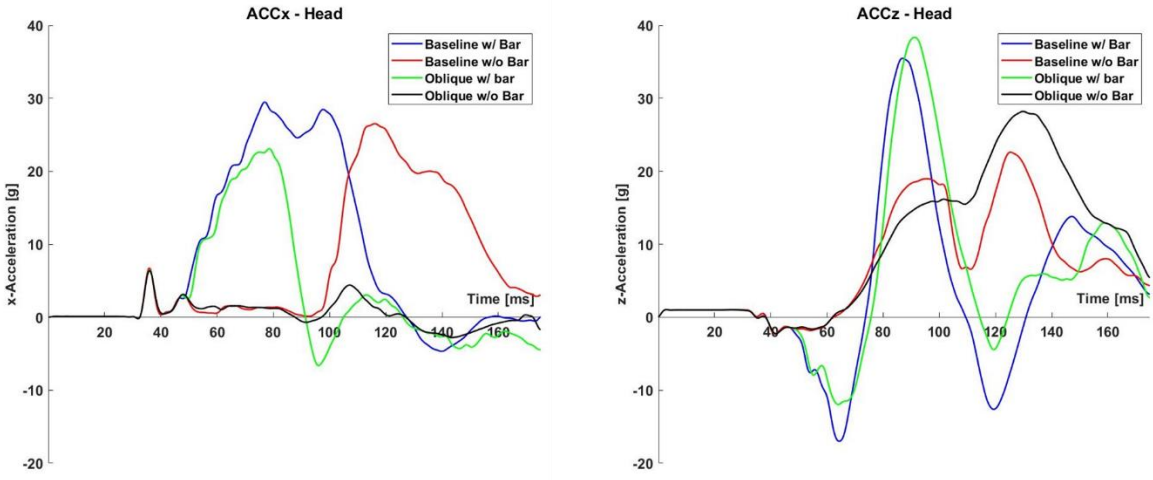

Figure B1: Head kinematics: X-acceleration [Left]; Z-acceleration [Right]

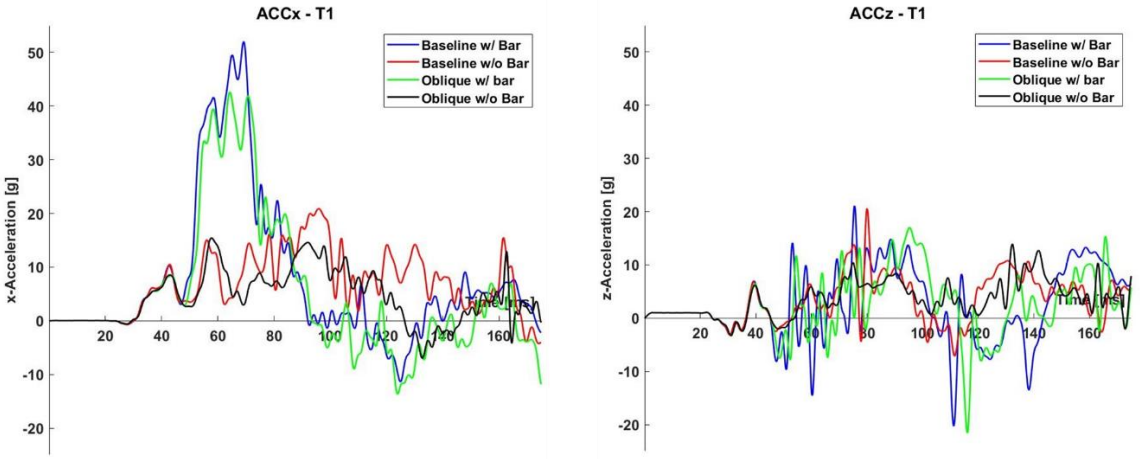

Figure B2: First thoracic vertebrae (T1) kinematics: X-acceleration [Left]; Z-acceleration [Right]

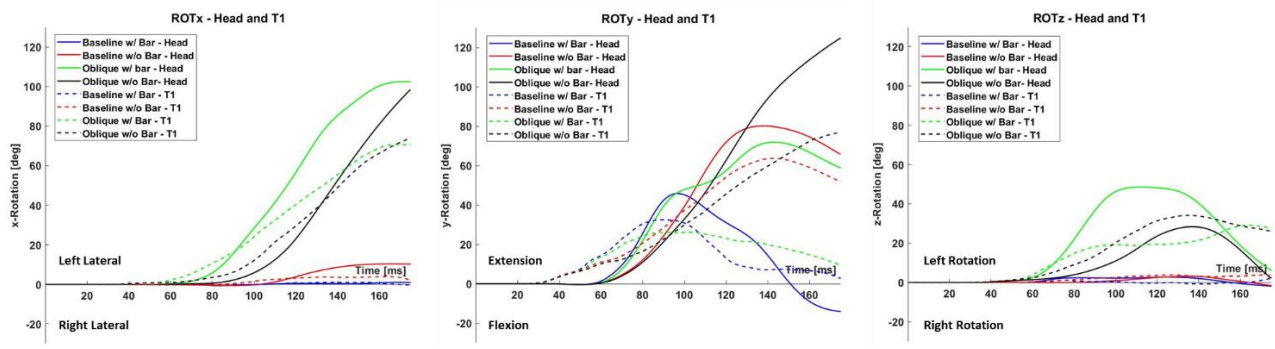

Figure B3: Head and first thoracic vertebrae (T1) kinematics: X-rotation [Left]; Y-rotation [Middle]; Z-rotation [Right]

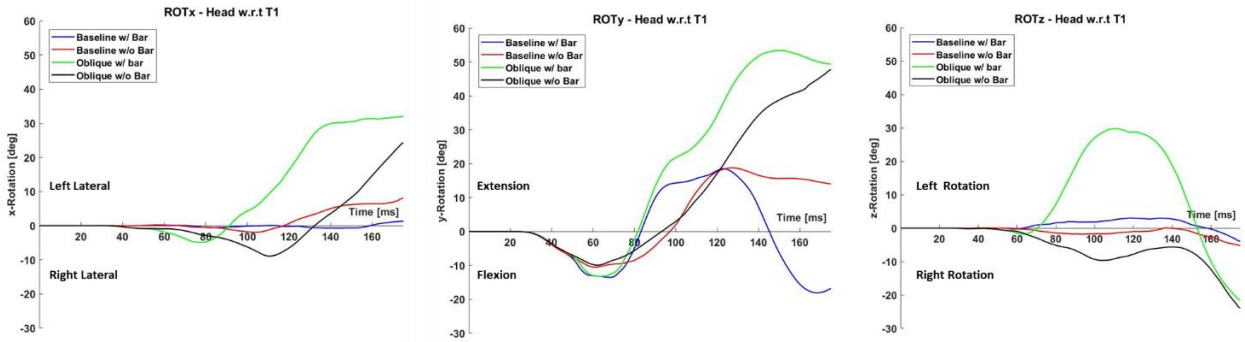

Figure B4: Head relative to first thoracic vertebrae (T1) kinematics: X-rotation [Left]; Y-rotation [Middle]; Z-rotation [Right]

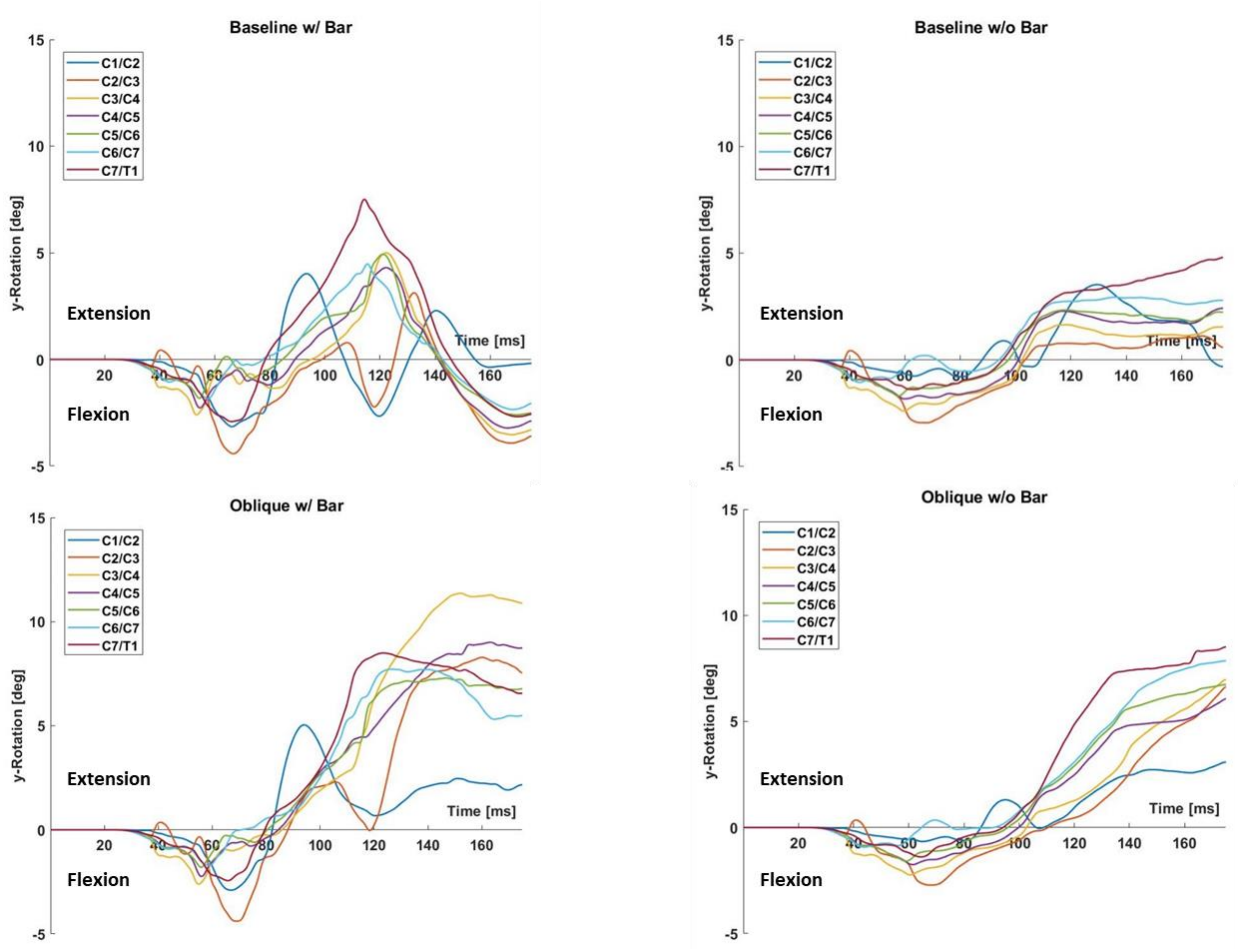

Figure B5: Intervertebral Kinematics

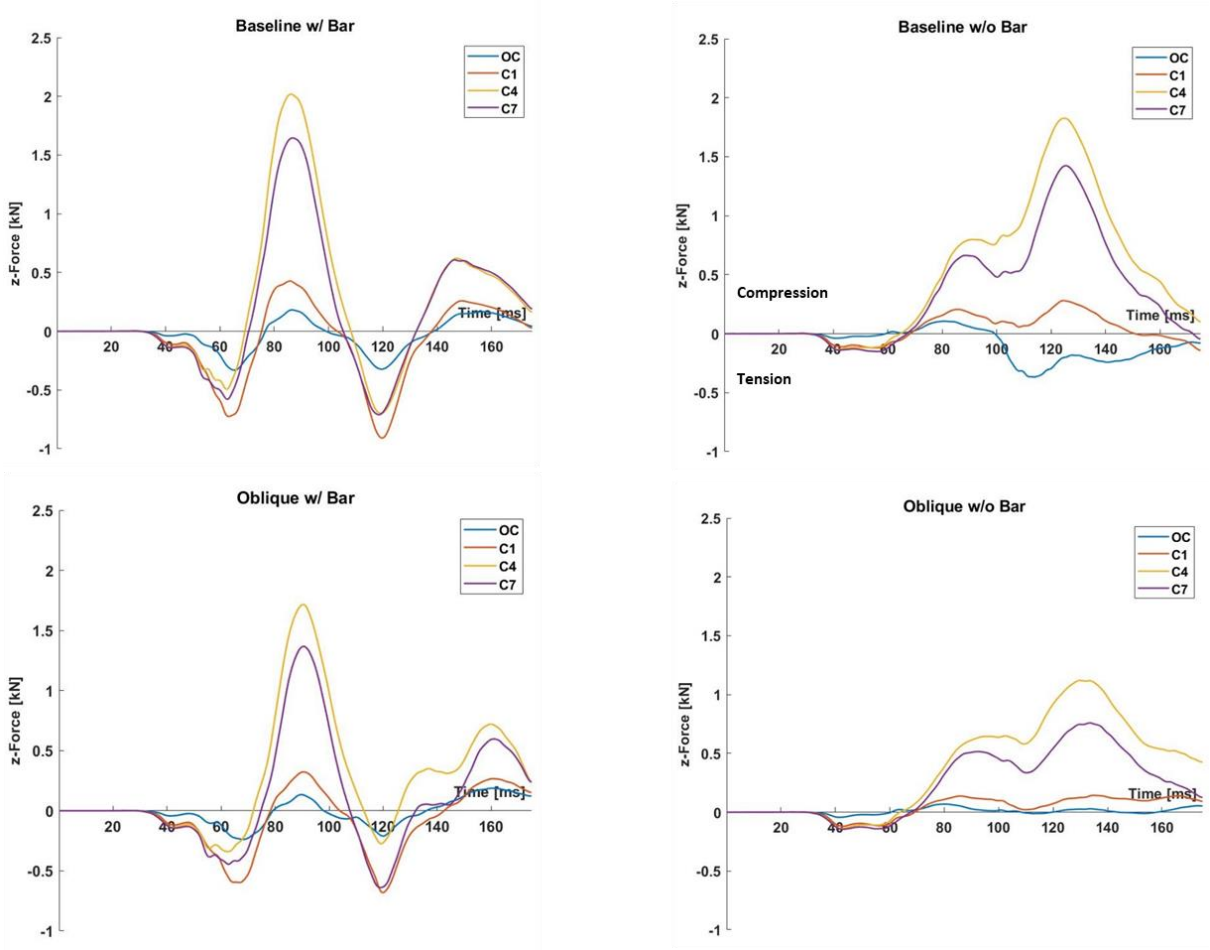

Figure B6: Intervertebral Forces

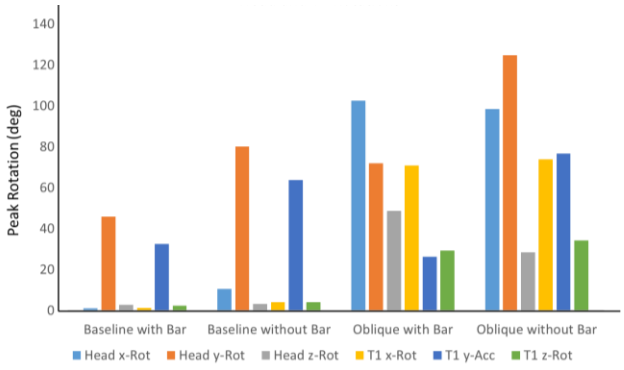

Figure B7. Magnitude comparisons: Head and first thoracic vertebrae (T1) rotations

Appendix C - GHBMC M50-O (Detailed) Model Kinematics

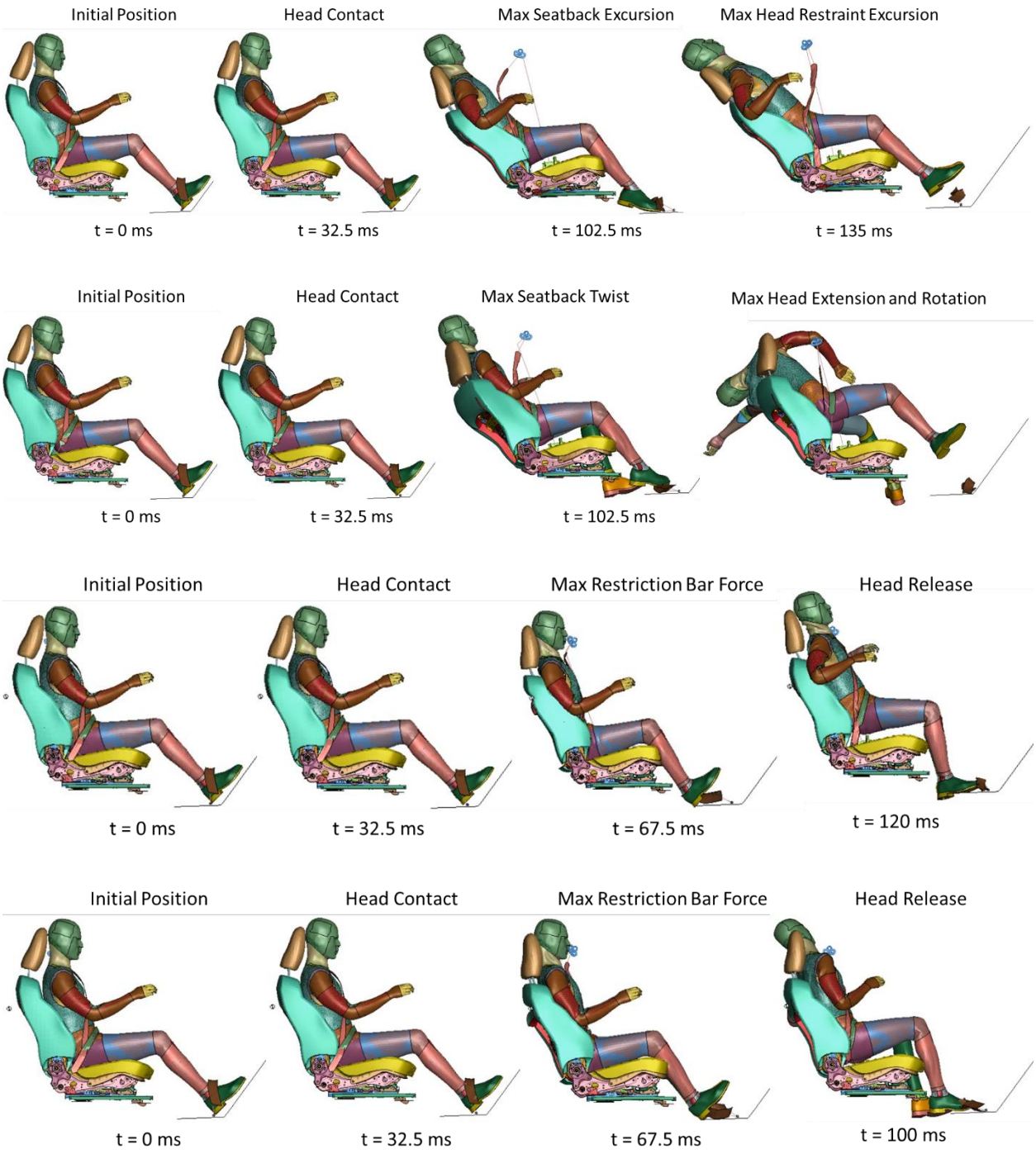

Figure C1. Representation of four different phases from each simulation; Top to Bottom: Baseline, Oblique, Baseline w/ Restriction Bar, and oblique w/ Restriction Bar